3. Numerical Simulation Reactor Research Project

Fusion plasmas are complex systems which involve a variety of physical processes interacting with each other across wide ranges of spatiotemporal scales. In the National Institute for Fusion Science (NIFS), we are utilizing the full capability of the supercomputer system, Plasma Simulator, and propelling domestic and international collaborations in order to conduct the Numerical Simulation Reactor Research Project (NSRP). Missions of the NSRP are i) to systematize understandings of physical mechanisms in fusion plasmas for making fusion science a well-established discipline and ii) to construct the Numerical Helical Test Reactor, which is an integrated system of simulation codes to predict behaviors of fusion plasmas over the whole machine range.

The Plasma Simulator was replaced to a new model (Fig. 1) in July 2020. It consists of 540 computers, each of which is equipped with 8 "Vector Engine" processors. The 540 computers are connected with each other by a high-speed interconnect network. The computational performance is 10.5 petaflops. The capacities of the main memory and the external storage system are 202 terabytes and 32.1 petabytes, respectively. The nickname of the Plasma Simulator is "Raijin (雷神)" which means a god of thunder.

Presented below in Figs. 2 and 3 are examples of successful results from collaborative simulation researches in 2020–2021 on the collisional merging process of field-reversed configuration (FRC) plasmas and on plasma shaping effects on ion temperature gradient (ITG) instability, respectively. Also, highlighted in the following pages are achievements of the NSRP on plasma fluid equilibrium and stability, energetic-particle physics, neoclassical and turbulent transport, plasma-wall interaction, and integrated transport simulation.

(H. Sugama)

Fig. 1 The Plasma Simulator, "Raijin (雷神)"

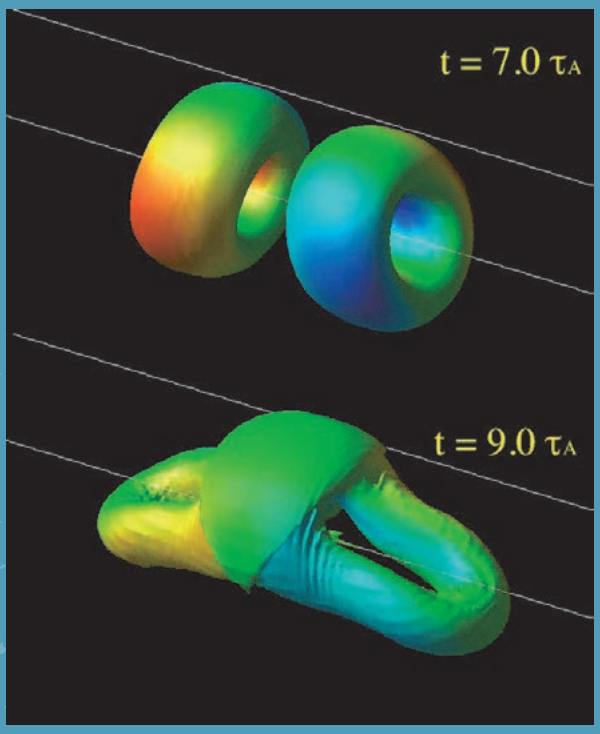

Fig. 2 Simulation results of the collisional merging process of field-reversed configuration (FRC) plasmas [presented by Dr. N. Mizuguchi (NIFS) collaborating with Nihon University]. The toroidal field strength on the isobaric surface is represented by color.

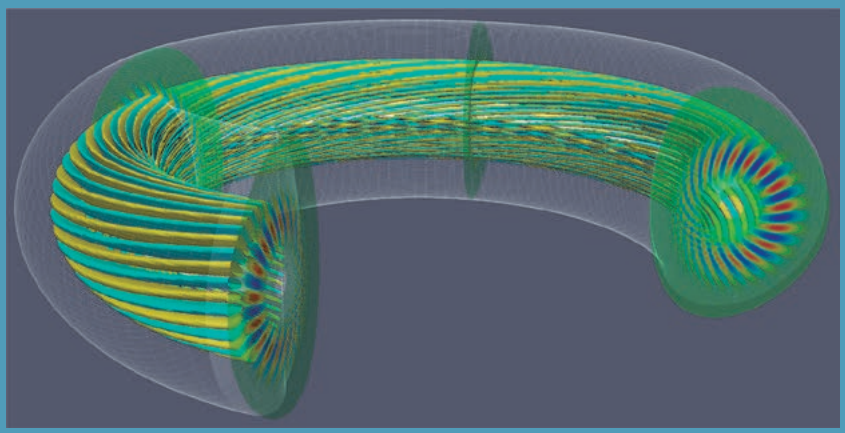

Fig. 3 Structure of the three-dimensional eigenfunction of the toroidal ITG mode obtained by the global gyrokinetic code (GKNET) for the non-circular tokamak configuration with the elongation $\kappa_0 = 1.5$ and the triangularity is $\delta_0 = 0.3$ [presented by Dr. K. Imadera (Kyoto University)]. Reference: K. Imadera *et al.*, Plasma Fusion Res. **15**, 1403086 (2020).

Progress of optimization scheme for magnetic field configuration

Highlight

A novel numerical optimization code of external-current system opens new window of stellarator/heliotron reactor concept

Stellarator/heliotron devices can confine hot plasma without driving net toroidal plasma current, owing to the twisted magnetic field generated by the external coil currents. Optimization of the magnetic configuration is one of the important issues in fusion plasma research based on the stellarator/heliotron concept because the magnetic configuration largely affects confinement of particle orbit, magnetohydrodynamic stability, micro-instability, edge plasma, etc. Conventional optimization of heliotron device is done by adjusting a small number of parameters describing a helical coil and comparing predicted plasma performances and engineering feasibility. For stellarator devices using modular coils, magnetic equilibrium is numerically optimized and external coils are designed to reproduce the optimized magnetic configuration.

A novel numerical optimization suite consisting of multiple numerical codes, OPTHECS, that can directly optimize the vacuum magnetic field/free-boundary equilibrium through modifying the shape and current of the external coils, has been developed. The developed code can not only treat the conventional parametric expression of helical coils but also cubic B-spline curve expression both of helical and modular coils, opening a new window of designing of stellarator/heliotron device. Using OPTHECS, it has been investigated if the magnetic configurations of advanced stellarators with robust divertor legs can be produced with helical coils. Fig. 1 shows a quasi-helically symmetric configuration obtained using OPTHECS. This configuration is realized using three helical coils and a pair of poloidal field coils. It has been found from the analysis of the field-line connection-length outside of the last-closed flux surface that the divertor legs exist in this configuration. The generation of divertor legs in other types of magnetic configurations with helical coils, including quasi-axisymmetric configuration and quasi-omnigeneous configuration, has also been found.

Application of OPTHECS to the improvement of the engineering design of heliotron-based fusion reactors has also started, taking advantage of the coil-based optimization scheme of the suite. Fig. 1 (c) shows the initial results of improved divertor clearance of a heliotron configuration obtained with helical coil expressed with a B-spline curve.

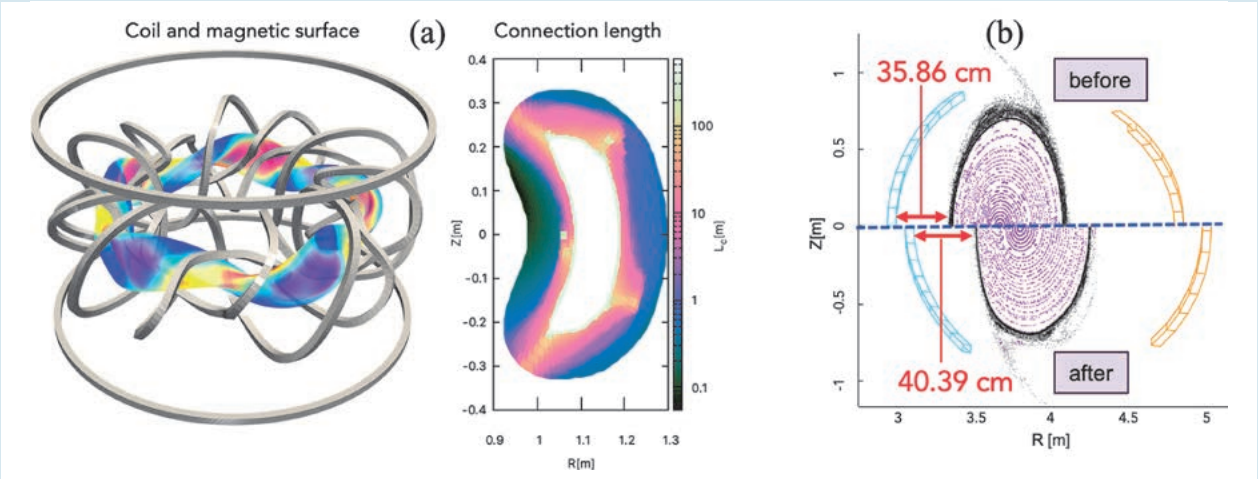

Fig. 1 (a) A quasi-helically symmetric configuration with helical coils obtained by OPTHECS. (b) Optimization of a heliotron configuration aiming at improved divertor clearance.

(H. Yamaguchi)

Transition from interchange mode to non-resonant mode in LHD collapse phenomena

In the MHD simulation of the LHD plasma collapse, a transition from $(m, n) = (3,3)$ interchange mode to (1,1) non-resonant mode is obtained, where m and n are the poloidal and toroidal mode numbers, respectively [1]. In the LHD experiment with the net toroidal current that flows so as to increase the rotational transform, collapses are caused by the (1,1) mode [2]. Thus, we examined the dynamics of the LHD plasma for the case with the net toroidal current. In the case that the rotational transform has the low shear profile in the core region and the value close to unity in the region, a transition occurs in the nonlinear evolution of the dynamics. In the end of the linear phase, the (3,3) mode is destabilized first as shown in Fig. 1(a). This mode is localized around the resonant surface and shows a typical interchange mode. Then, the dominant mode changes to the (2,2) component in the nonlinear evolution as shown in Fig. 1(b). Furthermore, the (1,1) component becomes dominant in the further nonlinear phase as shown in Fig. 1(c). Thus, the mode number of the dominant component decreases as in the case of the inverse cascade. Since the collapses are caused by the (1,1) mode in the experimental observation, this transition is considered as one of the candidates to explain the observed mode number.

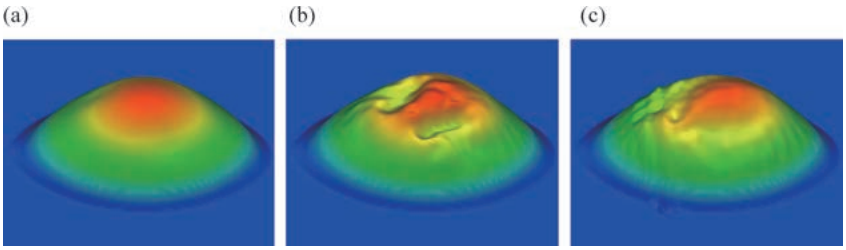

Fig. 1 Bird's eye view of the total pressure profile, (a) in the end of the linear phase, (b) in the early nonlinear phase and (c) in the further nonlinear phase.

[1] K. Ichiguchi *et al.*, submitted to Nucl. Fusion (2021).
[2] S. Sakakibara *et al.*, Nucl. Fusion, **55** 083020 (2015).

(K. Ichiguchi)

3D equilibrium study for a low shear stellarator with localized toroidal current density

Three-dimensional nonlinear MHD simulations study the core collapse events observed in a stellarator experiment. In the low magnetic shear configuration like the Wendelstein 7-X, the rotational transform profile is very sensitive to the toroidal current density. The 3D equilibrium with localized toroidal current density such as the ECCD (Electron Cyclotron Current Drive) is studied. If the toroidal current density follows locally in the middle of the minor radius, the rotational transform is also changed locally. For cases of 15 kA and 20 kA, the iota achieved to the unity, and then the topological change, where the magnetic island opens, is appeared.

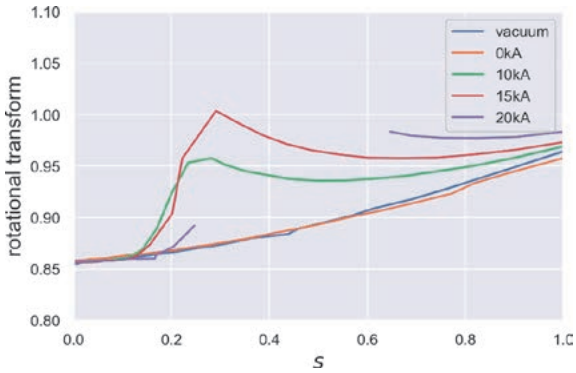

Fig. 2 Rotational transform profiles of the 3D equilibrium analyses for the sequence of the net toroidal current scan.

(Y, Suzuki)

Energetic-particle driven instabilities and energetic-particle transport in helical plasmas

Highlight

Precession drift reversal and rapid transport of trapped energetic particles due to an energetic-particle driven instability in the Large Helical Device

The effect of energetic deuterium ions with a distribution function consistent with a perpendicular neutral beam injection (NBI) was numerically investigated in a Large Helical Device (LHD) plasma reconstructed from a high-performance shot [1].

A fast growing m/n = 2/1 mode where m and n are poloidal and toroidal mode numbers, respectively is observed with its profile centered at the $\iota = 0.5$ radius. At the end of the linearly-growing phase, the mode saturates and its frequency chirps very rapidly and changes the sign. Fig. 1(a) shows the evolution of the mode amplitude and frequency, and the rapid frequency chirping can be seen in orange. This mode is important because it causes a rapid energetic particle perpendicular pressure redistribution, as can be seen in Fig. 1(b), where the pressure profile is shown for different times. It should be noted that the radial gradient of the energetic particle pressure profile even becomes positive for a short time after the saturation. An analysis of the energetic particle behavior shows that, at the start of the frequency chirping, a large portion of helically trapped energetic particles have their precession direction reverse. As shown in Fig. 1(c), the typical particle affected by this phenomenon reverses its precession drift direction, and at the same time is expelled from the plasma center, before going back to an equilibrium trajectory with the classical precession direction at a higher radius. The precession drift reversal is attributed to the poloidal ExB drift strong enough to counter the grad-B drift responsible for the precession drift motion, and at the same time a smaller radial ExB drift that pushes the particles from the center. This phenomenon is responsible for the energetic particle redistribution.

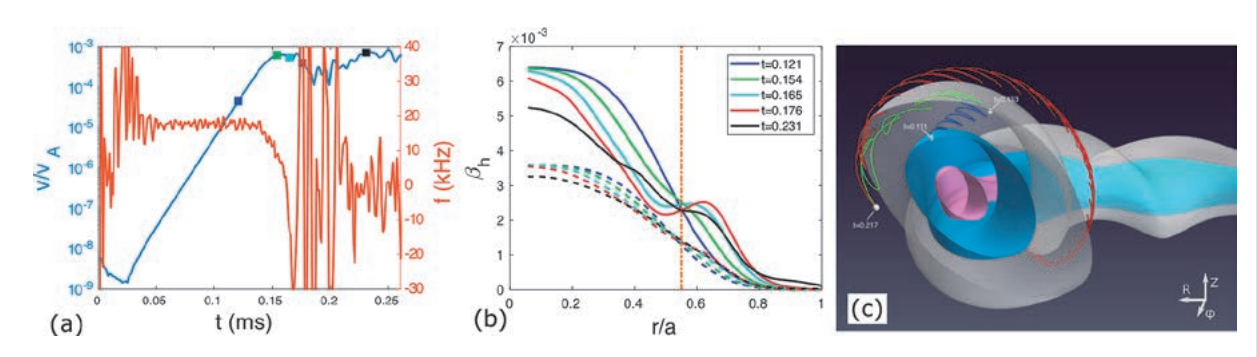

Fig. 1 (a) Time evolution of the radial plasma velocity amplitude of the mode shown in blue and the frequency in orange. The colored squares correspond to the different pressure profile times shown in Fig. 1(b). (b) Energetic particle pressure profiles for different times in the evolution. Solid (dashed) lines represent the perpendicular (parallel) energetic particle pressure profiles. (c) Trajectory of a typical energetic particle experiencing precession drift reversal. The blue line represents the trajectory at the end of the linear phase, the green curve during the drift reversal, and the red curve the return to an equilibrium trajectory at a higher radius.

[1] M. Idouakass *et al.*, "Numerical Observation of an m/n = 2/1 Mode with Strong Energetic Particle Redistribution in LHD", in the 29th International Toki Conference on Plasma and Fusion Research (2020).

(M. Idouakass)

Magnetohydrodynamic hybrid simulation of Alfvén eigenmodes in Heliotron J

Energetic-particle (EP)-driven MHD instabilities in Heliotron J, a low shear helical axis heliotron, were numerically investigated with MEGA, a hybrid MHD-EP simulation code [2]. The global Alfvén eigenmode (GAE) with poloidal/toroidal mode numbers m/n = 4/2 observed around r/a = 0.5 in the experiment was successfully reproduced; however, the energetic particle mode (EPM) with m/n = 2/1 at r/a>0.7 was not reproduced. Instead, an m/n = 2/1 GAE at r/a = 0.5 was weakly destabilized. For the initial EP distribution function (f_{h0}), the bump-on-tail and the slowing-down velocity distributions were considered. The bump-on-tail distribution reflects the experimental observation (high charge exchange loss), while the slowing-down distribution represents the ideal case. For the bump-on-tail case, the majority of the EP drive arises from the toroidicity-induced resonance for high-velocity particles. The contribution of the helicity-induced resonances is weaker because they are localized in the low-velocity region. These helicity-induced resonances are more significant for the slowing-down distribution. The different initial EP distributions also cause differences in the redistribution of EP pressure profile. The hollow (flat) EP pressure profile is formed after the saturation of the EP-driven MHD modes in the bump-on-tail (slowing-down) distribution.

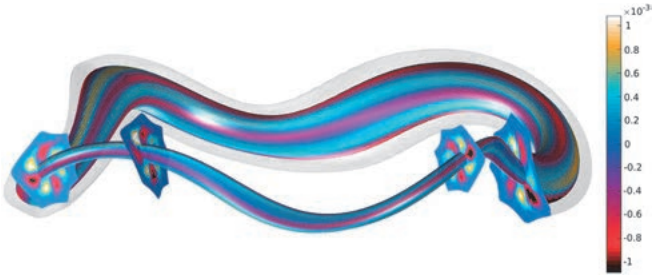

Fig. 2 Radial MHD velocity profile of the m/n=4/2 GAE in Heliotron J.

[2] P. Adulsiriswad *et al.*, Nucl. Fusion **60**, 096005 (2020).

(P. Adulsiriswad)

Hybrid Simulations of fast ion transport and losses due to the fast ion driven instabilities in the Large Helical Device

Hybrid simulations for energetic particles interacting with a magnetohydrodynamic (MHD) fluid were conducted using the MEGA code to investigate the spatial and the velocity distributions of lost fast ions due to the Alfvén eigenmode (AE) bursts in the Large Helical Device (LHD) [3]. The numerical fast-ion loss detector "numerical FILD" which solves the Newton-Lorentz equation was constructed in the MEGA code. Fast ions which are transported by the AE burst near the Last Closed Flux Surface (LCFS) were detected by the numerical FILD. Most of the fast ions detected by the numerical FILD are re-entering fast ions which re-enter in the plasma after passing through the outside of the plasma as shown in Fig. 3. The velocity distribution of lost fast ions detected by the numerical FILD is in good agreement with the experimental FILD measurements.

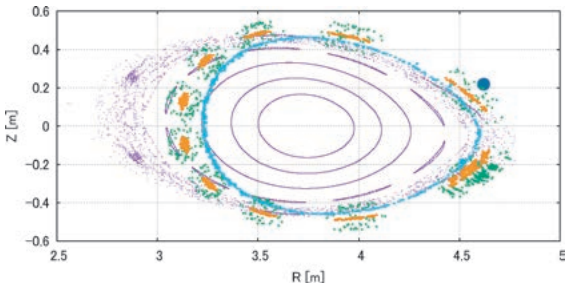

Fig. 3 Poincaré plots of fast ion orbits detected by the numerical FILD on the poloidal plane where the numerical FILD is installed. Gyro centers of a fast ion detected by the numerical FILD and the fast ion orbit before the AE burst are represented by yellow and blue dots, respectively. The Lorentz orbit of the detected fast ion is shown in green and the magnetic field lines are shown in purple. The blue circle represents the numerical FILD. The fast ion orbit represented by blue dots indicates that it is a re-entering particle.

[3] R. Seki *et al.*, "Hybrid Simulations of fast ion transport and losses due to the fast ion driven instabilities in the Large Helical Device", in the 28th IAEA Fusion Energy Conference (2021).

(R. Seki)

Theory, simulation, and modeling of turbulent transport

Highlight

Reduced models of turbulent transport in helical plasmas including effects of zonal flows and trapped electrons

Using transport models [1], the impacts of trapped electrons and zonal flows on turbulence in helical field configurations are studied. The effect of the trapped electrons on the characteristic quantities of the linear response for zonal flows is investigated for two different field configurations in the Large Helical Device. The turbulent potential fluctuation, zonal flow potential fluctuation and ion energy transport are quickly predicted by the reduced models for which the linear and nonlinear simulation results are used to determine dimensionless parameters related to turbulent saturation levels and typical zonal flow wavenumbers. The effects of zonal flows on the turbulent transport for the case of the kinetic electron response are much smaller than or comparable to those in an adiabatic electron condition for the two different field configurations. It is clarified that the effect of zonal flows on the turbulent transport due to the trapped electrons changes, depending on the field configurations. The nonlinear simulation results (NL) can be predicted by the reduced models for the ion heat transport for the case of the kinetic electron response in the inward shifted magnetic field configuration for the plasma parameters in Fig.1 [2]. These plasma parameters for the case of the kinetic electron response in the inward shifted magnetic field configuration are out of the range for constructing the reduced models.

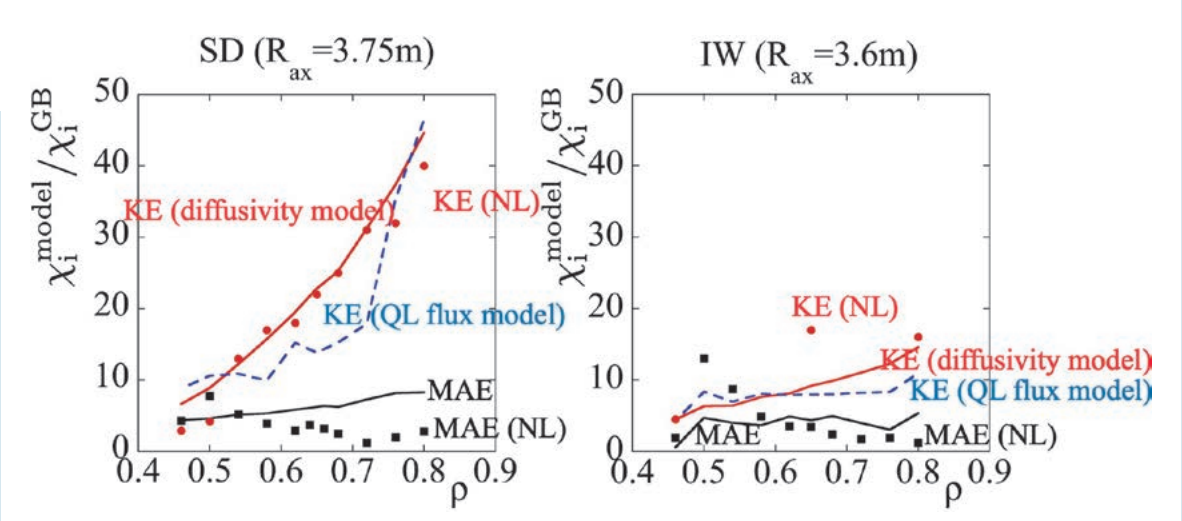

Fig. 1 The radial dependence of the normalized ion heat diffusivity is shown by the ion heat diffusivity model and the quasilinear (QL) flux model for the ion heat transport in the adiabatic (MAE) and kinetic electron (KE) conditions.

[1] S. Toda *et al.*, Phys. Plasmas **26**, 012510 (2019); doi: 10.1063/1.5058720.
[2] S. Toda *et al.*, M. Nunami, and H. Sugama, Journal of Plasma Physics **86**, 815860304 (2020); doi:10.1017/S0022377820000495.

(S. Toda)

Transport Prediction Scheme by Data Science and First-Principle Simulations

Transport of plasma heat and particle driven by the turbulence due to the micro-instabilities greatly affect the plasma confinement performances. The first-principle simulations based on the gyrokinetics are powerful to investigate the turbulent transport, not only qualitatively but also quantitatively. However, for the accurate estimate of the turbulences, a huge computational resources are demanded where we have to perform numerous numbers of the first-principle simulations for wide ranges of many physical parameters. Here, we have developed a new transport prediction scheme with as little as possible numbers of the first-principle simulations by using the technique of data science and the reduced transport model which approximately reproduces the turbulent transport levels. In the developed scheme, at first, we perform a mathematical optimization method of the techniques used in the data science for the reduced transport model to obtain the guesses of the input physical parameters needed for the first-principle simulation. Next, we perform the first-principle simulation under the guessed parameters. At last, based on the simulation result, we improve and optimize the transport model by employing the optimization technique again, we can obtain high accuracy transport model for each target plasma. See Fig. 2. The developed scheme enables us to perform the turbulent transport predictions with the minimum numbers of the first-principle simulations.

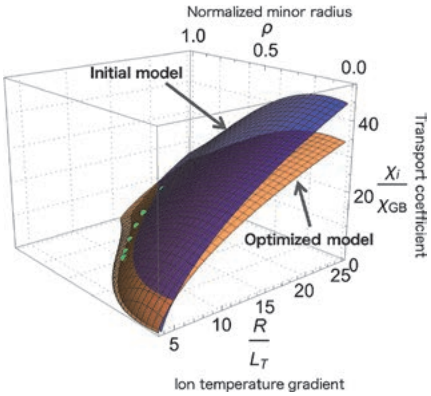

Fig. 2 Optimization of transport model by employing data science technique and the first-principle simulations. For the initial model (blue surface), a first-principle simulation at each radial position (green points) is performed and the optimized model (orange surface) is obtained.

(M. Nunami)

The variational formulation of the gyrokinetic system in general spatial coordinates

Gyrokinetics is a basic theoretical framework to study microinstabilities and turbulent processes in magnetized plasmas. Because background flow profiles are considered as one of the key factors for improving plasma confinement, momentum transport processes which determine the flow profiles are now being investigated extensively by large-scale gyrokinetic simulations. Thus, the momentum balance equation satisfied by the gyrokinetic model attracts our attention as a basis for theoretically and/or numerically investigating the physical mechanisms in the formation of the flow profiles. In the present work [3], our previous work [4] is extended to present the Eulerian variational formulation of the gyrokinetic system with electrostatic turbulence in general spatial coordinates and the invariance of the Lagrangian under an arbitrary spatial coordinate transformation is used to derive the gyrokinetic local momentum balance equation in an analogous manner to the theory of general relativity in which energy-momentum conservation laws are derived from the invariance of the action integral under arbitrary transformations of spatiotemporal coordinates. In the symmetric background magnetic field, the derived local momentum balance equation gives rise to the local momentum conservation law in the direction of symmetry. This derivation is in contrast to the conventional method using the spatial translation in which the asymmetric canonical pressure tensor generally enters the momentum balance equation. In the present study, the variation of the Lagrangian density with respect to the metric tensor is taken to directly obtain the symmetric pressure tensor, which includes the effect of turbulence on the momentum transport. In addition, it is shown in this work how the momentum balance is modified when the collision and/or external source terms are added to the gyrokinetic equation. The results obtained here are considered useful for global gyrokinetic simulations investigating both neoclassical and turbulent transport processes even in general non-axisymmetric toroidal systems.

[3] H. Sugama *et al.*, Phys. Plasmas **28**, 022312 (2021).
[4] H. Sugama *et al.*, Phys. Plasmas **25**, 102506 (2018).

(H. Sugama)

Numerical Simulations on Plasma-wall Interaction

Highlight

Simulations related to optical vortex — Molecular Dynamics simulation on Chiral Nano-Needle Fabrication by OV and Quasioptical simulation of OV beams in plasmas —

Omatsu group fabricated [1] chiral nanoneedles structure by vortex laser ablation. They used a ~2-mm-thick polished tantalum (Ta) as the target. Ta has a relatively low ablation threshold compared to other materials [2]. According their result [1], when the target Ta was irradiated with a circularly polarized Gaussian beam with the angular momentum quantum number $L = 0$ and the spin momentum quantum number $S = \pm 1$, no nanostructures, such as needles, were observed on the surface. In contrast, a linearly polarized optical vortex with $L = 0$ and $S = 0$ produced a chiral nanoneedle with a spiral conical surface at the center of the ablation zone. It is no exaggeration to mention that Omatsu's experiment is the start of research on optical vortex research in the field of optical physics. Against this backdrop, we used computer simulations instead of experiments to understand the interaction between light vortices and matter and addressed two issues: (1) molecular dynamics (MD) simulation on Chiral Nano-Needle Fabrication by optical vortex (OV) and (2) Quasioptical simulation of OV beams in plasma.

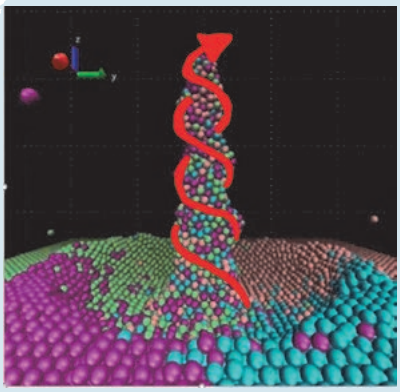

Fig. 1 Molecular Dynamics Simulation on Chiral Nano-Needle Fabrication. The red curve denotes the edge of the nanoneedle. It was found that a "ditch" is dug around the needle.

In the MD simulation on Chiral Nano-Needle Fabrication, the bcc Ta crystal at 300 K is prepared as the initial structure. We adopt EAM potential force field and NVT ensemble with Langevin thermostat [3,4]. We run the MD simulation with the external force field which is characterized by the Laguerre Gaussian beam [5]. As the result, we succeeded in fabrication of the chiral needle by the MD simulation (Fig. 1).

Next, the background of the quasioptical simulation of OV beams in plasmas is as follows: Kato et al. demonstrated [6] that a single free electron in circular motion emits twisted phones carrying orbital angular momentum. However, OV property of radiation was not discussed well up, even though the physics of electron cyclotron motion and its radiation is essentially used for plasma confinements, heating, and diagnostics. Therefore, we started numerical studies to understand the behavior of OV in dispersive plasmas. Using the quasioptical ray tracing code named PARADE [8], we showed [7] the first PARADE simulations of optical vortex beams in various plasma situations, and especially discuss the differences between optical vortex beams and conventional Gaussian beams in plasmas as shown in Fig. 2.

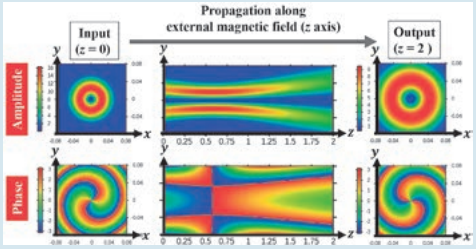

Fig. 2 Quasioptical simulation "PARADE" of OV beams in plasma. When an OV with Laguerre-Gaussian mode is input from $z = 0$, it propagates through the plasma along z axis which is parallel to the external magnetic field, and at $z = 2$ m, it becomes an output wave shown in the figures on the right. The upper figures show the amplitude distribution of the OV, and the lower ones show the phase distribution.

[1] K. Toyoda *et al.*, Phys. Rev. Lett., **110**, 143603 (2013).
[2] L. Torrisi *et al.*, J. Appl. Phys. **100**, 093306 (2006).
[3] H. Nakamura *et al.*, "Molecular dynamics simulation on structural formation of chiral nanoneedle by optical vortex", 38th JSST (2019).
[4] S. Habu and H. Nakamura, "MD Simulation on Chiral Needle Fabrication in Radiation Force Field of Laguerre Gaussian Beams", The 29th International Toki Conference (ITC29), 2020.
[5] L. Allen *et al.*, Phys. Rev. A, **45**, 8185 (1992).
[6] M. Katoh *et al.*, Phys. Rev. Lett. **118**, 094801 (2017).
[7] K.Yanagihara *et al.*, "Qusioptical simulation of optical vortex beams in plasmas", The 29th International Toki Conference (ITC29), 2020.
[8] K. Yanagihara *et al.*, Phys. Plasmas **26**, 072112 (2019).

Development of Simulation Codes to Treat Hydrogen Molecules Process in Divertor Plasma Region including Divertor Plate

By combining the following three simulation codes, *i.e.*, (i) the Neutral-Transport code with the rovibrationally resolved Collisional-Radiative model (NT-CR) [9], (ii) EMC3-EIRENE code [10], and (iii) the Molecular Dynamics (MD) simulation [11], we successfully calculated each hydrogen molecule (H2) population with vibrational state (v) and rotational state (J) at any position for carbon or tungsten divertor plate [12]. Neutral transport codes are widely used to analyze divertor plasmas. However, the H_2 rovibrational population is not considered. Using our codes, we calculated the H_2 rovibrational populations for a certain LHD plasma with carbon divertor plates.

As shown in Fig. 3, we found that the J-dependence of each H_2 population for v = 0,1,2 near the divertor plate becomes the Boltzmann distribution, which is consistent with the estimation by emission spectroscopy of the Fulcher-α band of H_2 in LHD [13].

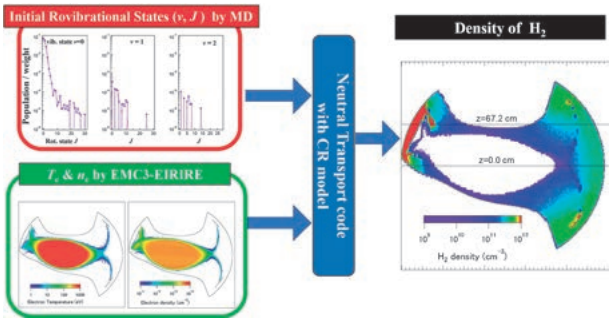

Fig. 3 Concept of the hybrid simulation among molecular dynamics, EMC3-EIRENE and Neutral-Transport code with the rovibrationally resolved Collisional-Radiative model.

[9] K. Sawada and M. Goto, Atoms **4** (2016) 29.
[10] G. Kawamura *et al.*, Plasma Phys. Control. Fusion **60** (2018) 084005.
[11] S. Saito *et al.*, Contrib. Plasma Phys. (2020) e201900152.
[12] K. Sawada *et al.*, Contrib. Plasma Phys. (2020) e201900153.
[13] H. Ishihara *et al.*, J. Quant. Spectrosc. Radiat. Transf., **267** (2021) 107592.

Structural Change of Tritium-substituted Macromolecules by β decays

A human telomeric DNA structure is found at the end of eukaryotic chromosomes and consists of a specific repeating base sequence (TTAGGG) and various proteins. It has been reported that telomere shortening can cause atherosclerosis and cancer. Adopting the nucleotide sequence of telomeric DNA, *i.e.*, TCTAGGGTTAGGGTTAG, we investigate the effect of tritium β decay on telomeric DNA by molecular dynamics (MD) simulation. In paticula, we focus on both the hydrogen bond [15] and the covalent bond breaking in the telomere structure. For the latter purpose, we used the dynamic reactive force field (ReaxFF) [14], which is known to be able to handle covalent bond breaking.

In order to investigate the effect of the β decay on covalent bonds, we assume that the two hydrogens covalently bonded to the carbon at the 5′ position of the sugar were decayed to helium (described as a scratch). When a lot of scrateches are input to telomeric DNA, Fig. 4 shows snapshots at 1.85 ns from the initial structure. Furthermore, it also shows that covalent bond breaking has occurred and the structure is split into about three pieces. Thus, it was confirmed that when the number of scratches increases, the covalent bonds are broken and the telomere structure collapses.

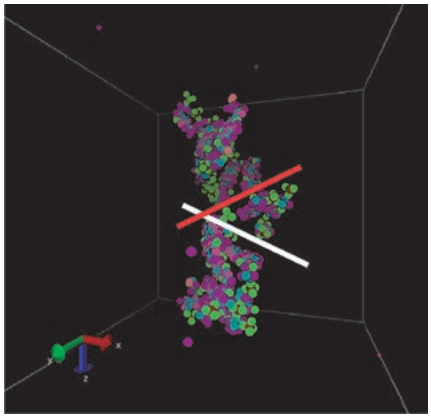

Fig. 4 A snapshot of the telomeric DNA structure at 1.85 ns after the initial structure. Figure shows that the double helix structure of the initial structure is broken into three pieces. For clarity, the broken parts are described with red and white lines.

[14] van Duin *et al.*, J. Phys. Chem. A, **105**, 9396 (2001).
[15] H. Nakamura *et al.*, Jpn. J. Appl. Phys. **59**, SAAE01 (2020).

Integrated Transport Analysis based on Data Assimilation Technique

Highlight

Data assimilation technique has made progress on a "whole-discharge" transport modelling of LHD plasmas

A data assimilation technique has been implemented into the integrated transport analysis suite, TASK3D [1], to make a transport model to be suitable for the actual plasmas, and then to predict and control the fusion plasmas [2]. The system is named as ASTI (Assimilation System for Toroidal plasma Integrated simulation). The temporal variations along with the change of profiles of the ion and electron temperatures have been successfully demonstrated by ASTI for an actual discharge of the Large Helical Device (LHD) (as shown in Fig. 1). Now, the ASTI development has been progressing towards controlling plasmas by implementing the new scheme, in addition to assimilate the measurement data. This will open up the new phase of general data assimilation methodology.

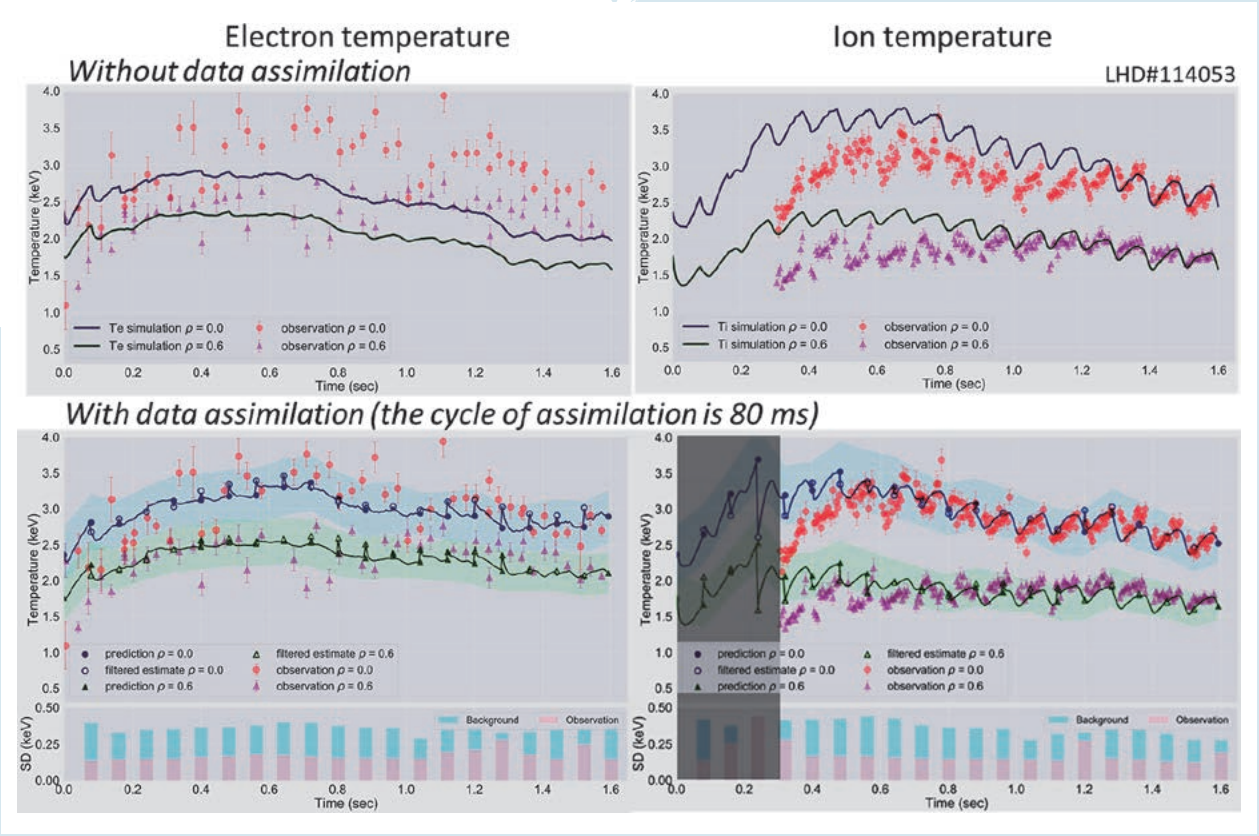

Fig. 1 Temporal change of electron (left) and ion (electron) temperatures at the plasma center (red dots with error bars for measurement and blue curve for simulation), and at 60% of the average minor radius (purple dots with error bars for measurement and green curve for simulation) for LHD discharge 114053. The upper column is for TASK3D only (without data assimilation), and the lower column is for ASTI (with data assimilation). Hatched region at the right-bottom is a part where the electron temperature is assimilated because the ion temperature measurement was not performed. The bars in the lower panels indicate the estimated standard deviations (SD) of the background error and observation noise before filtering.

The data assimilation technique is one of the statistical estimation methodologies. It has been widely developed and practically employed in meteorology and oceanology (weather forecast, prediction of El Niño and La Niña).

The time-series measurement data (profiles of the ion and electron temperatures) for a whole discharge of LHD experiment are assimilated into TASK3D in which one-dimensional diffusive heat transport equation is solved for ions and electrons. Here, previously obtained turbulent transport model, gyro-Bohm (for electrons) and gyro-Bohm-gradTi (for ions) models are employed in TASK3D. Utilizing the data assimilation technique, the state vector composed of physics variables (as shown in Fig. 2; notations are given in the figure caption) is estimated with employing the ensemble Kalman filter (EnKF) [3]. This prediction (TASK3D) and filtering processes make the given transport model to be adapted for the actual plasma behaviors. ASTI can also be used to estimate the variables not observed and the model parameters that can explain observed time series data. The ensemble Kalman smoother (EnKS), a data assimilation method for analysis, has also been implemented in ASTI [4].

Figure 2 shows the data assimilation results of the ion and electron temperatures in comparison to the results without the data assimilation ("usual" TASK3D simulation) for a particular LHD discharge (discharge number: 114053) as a whole. The implemented transport model is found not to be satisfactory to predict temporal variations of temperatures, but the data-assimilation can provide reasonably well alignment to the measured data. This is realized by "optimizing" the transport model to be suitable for the actual situations.

Now, it has been progressing towards data assimilation for a group of discharges so that widely applicable transport model is obtained, and in the meantime, towards "the ASTI for the control" for actual plasma control to be demonstrated.

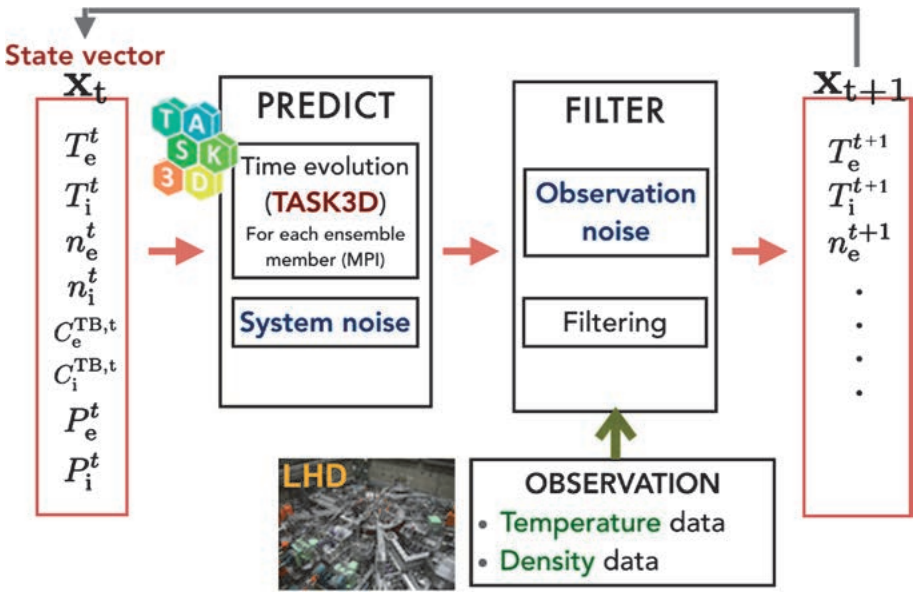

Fig. 2 A data assimilation scheme based on TASK3D and EnKF. Here, the state vector is composed of T (temperature), n (density), C^{TB} (coefficient of turbulent transport model) and P (NBI (neutral beam injection) heat deposition), with suffixes, e and i, for electrons and ions, respectively.

[1] S. Murakami *et al.*, Plasma Phys. Control. Fusion **57**, 119601 (2015).
[2] Y. Morishita *et al.*, Nucl. Fusion **60**, 056001 (2020).
[3] G. Evensen, Ocean Dyn. **53**, 343–67 (2003).
[4] Y. Morishita *et al.*, Plasma and Fusion Research **16**, 2403016 (2021).

(Y. Morishita, Kyoto University)